



HAL
open science

Quantum dynamics of O 17 in collision with ortho- and para- O 17 O 17

Grégoire Guillon, Maxence Lepers, Pascal Honvault

► **To cite this version:**

Grégoire Guillon, Maxence Lepers, Pascal Honvault. Quantum dynamics of O 17 in collision with ortho- and para- O 17 O 17. *Physical Review A*, 2020, 102 (1), pp.012810. 10.1103/PhysRevA.102.012810 . hal-02953726

HAL Id: hal-02953726


<https://hal.science/hal-02953726v1>

Submitted on 8 Dec 2020

HAL is a multi-disciplinary open access archive for the deposit and dissemination of scientific research documents, whether they are published or not. The documents may come from teaching and research institutions in France or abroad, or from public or private research centers.

L'archive ouverte pluridisciplinaire **HAL**, est destinée au dépôt et à la diffusion de documents scientifiques de niveau recherche, publiés ou non, émanant des établissements d'enseignement et de recherche français ou étrangers, des laboratoires publics ou privés.

Quantum dynamics of ^{17}O in collision with ortho- and para- $^{17}\text{O}^{17}\text{O}$

Grégoire Guillon¹,* Maxence Lepers¹, and Pascal Honvault¹*Laboratoire Interdisciplinaire Carnot de Bourgogne, UMR CNRS 6303, Université de Bourgogne Franche-Comté 21078 Dijon Cedex, France* (Received 18 April 2020; accepted 24 June 2020; published 16 July 2020)

We report full quantum scattering cross sections for the peculiar $^{17}\text{O} + ^{17}\text{O}^{17}\text{O}$ system, at relatively low collision energies. We consider different types of collision-induced transitions, as the indistinguishability of the three nuclei allows for the mixing of reactive, inelastic, and elastic processes. Furthermore, due to the nonzero nuclear spin of ^{17}O and the existence of nuclear spin isomers ortho- and para- O_2 , we pay particular attention to transitions between these two species, that is, the ortho-para conversion process. We find that the corresponding cross section has a magnitude comparable to that of the $\text{H}^+ + \text{H}_2$ counterpart.

DOI: [10.1103/PhysRevA.102.012810](https://doi.org/10.1103/PhysRevA.102.012810)

I. INTRODUCTION

Oxygen, with three stable isotopes ^{16}O , ^{17}O , and ^{18}O , with abundances 99.76%, 0.04%, 0.20%, and nuclear spins $s = 0$, $s = 5/2$, $s = 0$, respectively, plays an important role in atmospheric elementary as well as complex chemical processes, and O_2 is the next but most abundant molecule in the atmosphere, after nitrogen N_2 . The upcoming oxygen compound in complexity, ozone O_3 , which absorbs a huge amount of UV radiation from the sun in the stratosphere, is mainly formed from metastable states of excited transient complex O_3^* of the $\text{O} + \text{O}_2$ reaction, eventually stabilized. Many studies have thus been dedicated to the measurement [1] or calculation [2] of rate constants for this so-called oxygen exchange reaction. To facilitate measurements and in relation to the secular mass-independent fractionation problem of ozone [3], these studies have focused on isotope effects, replacing ^{16}O by ^{18}O (most often) or ^{17}O in the atomic (O) [2,4,5] or molecular (O_2) [6,7] species. Totally symmetric systems with zero total nuclear spin, such as $^{16}\text{O} + ^{16}\text{O}^{16}\text{O}$ and $^{18}\text{O} + ^{18}\text{O}^{18}\text{O}$ have also been theoretically explored [6,8], giving in particular much larger cross sections, hence much faster rate constants.

In relation to another completely different field, the O_2 molecule in its ground $^3\Sigma_g^-$ state has been a subject of interest in itself, as a prototype of simple open-shell paramagnetic species approaching a Hund's case (b), in the context of buffer gas loading and evaporative cooling experimental techniques, for subsequent magnetic trapping [9]. The study of the ratio of rates for elastic to inelastic collisions of the target molecule with a rare gas atom (most often ^3He because of its higher vapor pressure at sub-Kelvin temperatures than ^4He) at very low collision energies is important in this context for the optimization of the parameters of the experiment. The particular $^{17}\text{O}^{17}\text{O}$ diatom has been among the first molecules to be proposed as a serious potential candidate for cooling and trapping in the view of the obtaining of cold molecular samples [9–14]. It has been shown to be much more adapted [12,15,16] than $^{16}\text{O}^{16}\text{O}$ and $^{18}\text{O}^{18}\text{O}$ because of the possibility

of population of the ground rotational level $j = 0$ (or $N = 0$ in the context of cold molecules), leading to stability with respect to evaporative cooling and avoiding losses, which is precisely forbidden in the two other zero nuclear spin isomers. The possible ortho-para or para-ortho conversion of $^{17}\text{O}^{17}\text{O}$ that might happen when encountered with residual O atoms in the O_2 beam or trap may be of importance in this context of cold chemistry, as it may change the parity of the rotational quantum number j , the fine structure associated to it, and might lead to trap loss. Therefore, the findings reported in this paper might serve as a preliminary result toward a more refined description, even if, as we shall describe in the next section, the fine structure of O_2 ought to be considered for a complete study of this process at low energies.

We present here a theoretical study of the $^{17}\text{O} + ^{17}\text{O}^{17}\text{O}$ reaction, thereafter systematically abbreviated as $7 + 77$, involving nonzero nuclear spin totally symmetric $^{17}\text{O}^{17}\text{O}^{17}\text{O}$ (777) complex as an intermediate. In addition to the existence of two diatomic nuclear spin isomers ortho- $^{17}\text{O}^{17}\text{O}$ ($o77$) and para- $^{17}\text{O}^{17}\text{O}$ ($p77$), this reaction allows for the possibility of ortho-para interconversion which is not arising from hyperfine structure couplings, as could possibly happen in a strongly inhomogeneous magnetic field.

The 777 isotopomer of ozone is of course the rarest, due to the extremely low natural abundance in ^{17}O . As a consequence, the $7 + 77$ process is not such as to be relevant in an atmospheric context. Nevertheless, as a prototype for a fully symmetric three-particle system with nonzero total nuclear spin, it sheds light on physics of processes involving indistinguishable entities.

II. THEORY

As in all our previous studies, we basically assume in this paper that no nuclear spin-dependent terms are included in the Hamiltonian governing the dynamics of the nuclei. This is entirely justifiable, given the very low magnitude of the nuclear magneton.

As we are considering collision energies in the range [1,10] meV, it seems reasonable to also neglect fine structure and magnetic interactions due to electronic spin of open-shell O

*gregoire.guillon@u-bourgogne.fr

(3P_g) and O_2 ($^3\Sigma_g^-$) in their ground state [17–21]. In fact, for the lowest collision energies, the spin-spin interaction coupling constant in O_2 , being roughly of 0.25 meV, is not entirely negligible, being in particular higher than the rotational constant of 0.18 meV, while the spin-rotation constant of -0.001 meV seems to be. But we definitely neglect transitions between rotational sublevels correlating to a pure Hund's case (b) as described in Ref. [17] and Ref. [21]. On the side of the O atom, the spin-orbit interaction of roughly 20 meV is not completely negligible either, but has been accounted for in the potential energy surface (PES) we use, which switches at long range to an accurate multipolar expansion including the fine structure of O and O_2 [22].

On the other hand, the nuclear spin of ^{17}O plays a key role, in an indirect way, in connection with the spin-statistics theorem, or Pauli principle. Indeed, it has the effect of relentlessly constraining the nuclear motion. This in turn results in dramatically changed cross sections when compared to the situation when spin symmetry is neglected, as we have shown in the case of zero nuclear spin for oxygen ^{16}O or ^{18}O [6,8].

The $7 + 77$ collision system is of $X + X_2$ type, as were the previously studied processes $6 + 66$ and $8 + 88$. The main difference with the latter is that the spin of the ^{17}O nucleus is not zero anymore (for ^{17}O $s = 5/2$), and thus the total nuclear spin S does not reduce to zero as was the case for $6 + 66$ and $8 + 88$. Also ^{17}O nuclei are fermions and thus subjected to Fermi-Dirac spin statistics. As for the $6 + 77$ system [7], the entrance channel is still defined in reference to the 77 spin species, that is, we can have either $7 + o77$ or $7 + p77$. At this point, we see that there is already a constraint on the acceptable spin functions of the 777 complex in the entrance channel. Furthermore, we need to separate cross sections between components of a given symmetry species (which is the space symmetry for the motion of nuclei), based on the restrictions imposed by the different symmetries of nuclear spin functions, in agreement with the Pauli principle. Finally, we have to properly enumerate the number of nuclear spin functions of each allowed symmetry to obtain spin weights for different symmetry cross sections. All relevant details are explicit in Appendixes A and B.

The formalism we base upon to obtain dynamical observables is time-independent quantum mechanics (TIQM). We solve the time-independent Schrödinger equation by expanding the nuclear wave function in terms of body-fixed democratic hyperspherical harmonics. Full details of the method can be found in Ref. [23]. The correct symmetry cross sections are obtained with a proper choice of hyperspherical harmonics included in the expansion, respecting the constraints brought by the operations of the S_3 permutation symmetry group [24].

Numerical computations are supported by a recently developed PES, referred to as the DLLJG PES, after the names of its authors [25]. The PES is extrapolated in the $O + O_2$ asymptotic region using the quadrupole-quadrupole and van der Waals interactions calculated in Ref. [22]. This latest PES has been shown to give observables in good agreement both in the fields of high-resolution vibrational spectroscopy and, more recently, reactive molecular dynamics. Our group has already used it on previous scattering calculations, for example, with the $6 + 66$ [6] and $8 + 88$ [8] systems. We have chosen collision energies ranging from 1 to 10 meV, as

this is the domain where most resonances occur and where the most pronounced difference in behaviors between $o77$ and $p77$ is expected. Moreover, higher energies would only be of use for the calculation of rate constants at temperatures relevant for stratospheric ozone, which is somewhat pointless in the present study. We selected a maximal value $\Omega_{\max} = 40$ for the projection of the total angular momentum on the least inertia axis of the 777 complex. This has proved after various numerical tests to yield well-converged results. We have initially included 100 channels at $J = 0$ for the computation of A_1 and A_2 symmetry cross sections (see Appendix B) and 200 channels for the computation of E symmetry cross sections. This allows for the inclusion of vibrational quantum numbers of the diatom 77 up to $v = 4$. The maximum value of total angular momentum we used is $J_{\max} = 45$, sufficient for this relatively low-energy domain. The close-coupled equations in the hyper-radius have been solved with the help of the so-called Johnson-Manolopoulos log-derivative propagator [26,27]. The reactance matrix was obtained by matching the propagated solution to the form imposed by the boundary conditions of a scattering problem [23]. Integral cross sections are then readily obtained from it.

III. RESULTS AND DISCUSSION

We show in this section both state-to-state and initial state-selected integral cross sections (ICSs) for the $7 + o77$ and $7 + p77$ collision processes.

As in our previous works on the $6 + 66$ and $8 + 88$ systems involving three identical nuclei, the classical view of bond breaking and reforming during the “reaction” is blurred. So we have to distinguish between the (energetically) elastic, the (energetically) nonelastic, and the total process cross sections. In the elastic process, products, which are identical with reagents, are found in the exact same quantum state after scattering. In the nonelastic one, products exit the reaction in a quantum state differing from that of the reagents by at least one quantum number. The total process is the sum of the former two. In this paper, we will restrict ourselves to the case of an initial vibrational level set equal to $v = 0$. For this low-energy range, the products will obviously remain in this vibrational level $v' = 0$, and we shall not mention this quantum number anymore.

We will first focus on specific state-to-state transitions, especially when it comes to possible ortho-para (o-p) or para-ortho (p-o) conversions. We will then show overall cross sections for transitions toward all accessible outcomes compatible with the collision energy, including the weight factor brought by the possibility of numerous spin functions.

Figure 1 shows, for the $7 + o77(j = 0)$ process, pure state-to-state cross sections (regardless of the spin factors) associated with the first three o-p transitions allowable in this energy range. They are plotted as a function of collision kinetic energy, from 1 to 10 meV. All processes, being endothermic, present a threshold, but the one for the transition $j = 0 \rightarrow j' = 1$ appears at an energy too low to be apparent here, the rotational constant of 77 being around 0.17 meV [28].

So, as a global tendency, ICSs rise sharply to a maximum, then progressively decrease and seem to converge to a common almost constant value, below $20 a_0^2$ at the highest

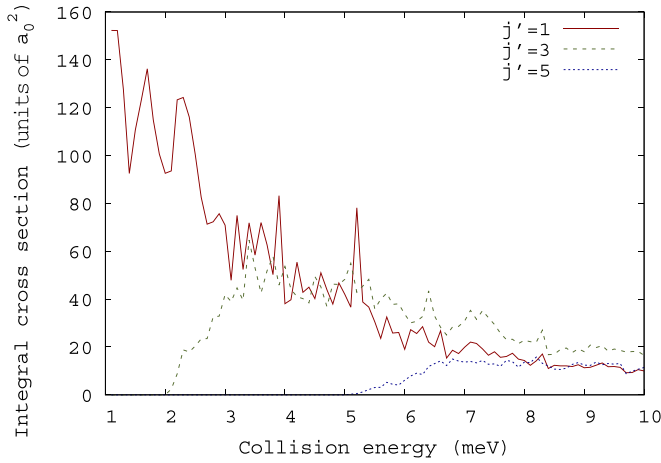


FIG. 1. State-to-state integral cross sections (in the unit of a_0^2), as a function of collision energy, for the reactive ortho-para conversion process $7 + \text{o}77(j=0) \rightarrow 7 + \text{p}77(j')$ with $v=0$. The first three values of j' are shown. Spin weights are not included.

energies. ICSs for the $j=0 \rightarrow j'=1$ process exhibit very marked oscillations at low energies and can reach values as high as $150 a_0^2$. These resonance structures, constituting a massif of narrow peaks and troughs in the ICS, are mainly shape resonances characteristic of long-lived metastable states supported by a deep well (1.13 eV) in the PES. This general behavior has already been observed for the $\text{H}^+ + \text{H}_2$ o-p transition [29] with a well four times as deep. Also the values of state-to-state ICSs for the present system are of the same order of magnitude as for $\text{H}^+ + \text{H}_2$.

Figure 2 presents, this time for the $7 + \text{p}77(j=1)$ collision, pure state-to-state cross sections corresponding to the reverse p-o processes, starting from the p77 species, for the same energy range. In this reaction, as we expect for a barrierless entrance channel, there is of course no threshold for the exothermic $j=1 \rightarrow j'=0$ process. In fact, for lower energies than those presented here, the $j=1 \rightarrow j'=0$ process

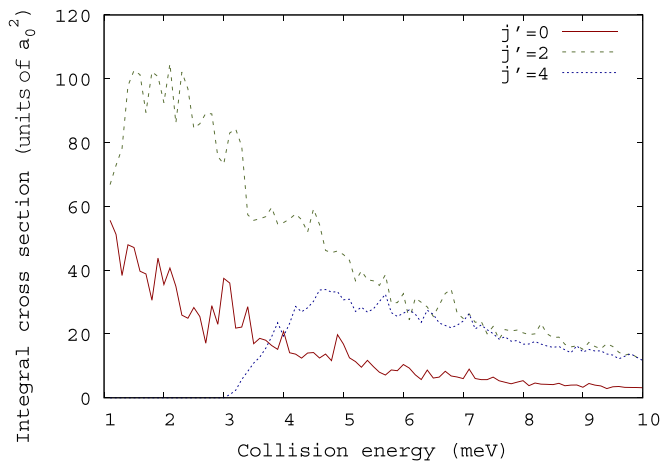


FIG. 2. State-to-state integral cross sections (in the unit of a_0^2), as a function of collision energy, for the reactive para-ortho conversion process $7 + \text{p}77(j=1) \rightarrow 7 + \text{o}77(j')$ with $v=0$. The first three values of j' are shown. Spin weights are not included.

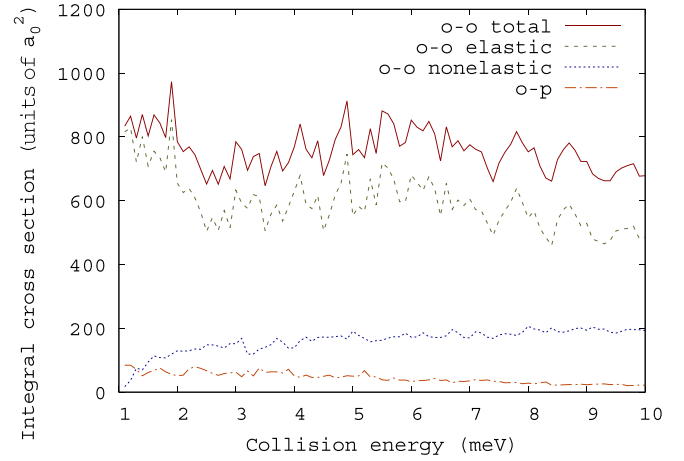


FIG. 3. Spin-averaged initial state selected integral cross sections (in the unit of a_0^2), as a function of collision energy, for the reactive process $7 + \text{o}77(j=0)$ with $v=0$.

would likely dominate the $j=1 \rightarrow j'=2$ process. But for the [1,10] meV energy range reported here, it appears the latter mentioned transition lies above all other allowable p-o conversions. We also notice that in this case, the ICSs oscillations are much less marked than for the o-p process. This is because, for the latter, additional Feshbach resonances are occurring, due to the coupling with bound states belonging to above closed channels, waiting to be open at threshold energies, and absent from the present exothermic $j=1 \rightarrow j'=0$ transition. The maximum value of the highest ICS (for the $j=1 \rightarrow j'=2$ process) is barely $100 a_0^2$. Also, the exothermic process $j=1 \rightarrow j'=0$ seems to tend to a very low value, a shade above zero, at the highest collision energies. The ICS for the $j=1 \rightarrow j'=4$ has the same global shape as those described above. It shows nevertheless more damped oscillations, and presents a threshold at around 3 meV. It seems to take values extremely close to that for the $j=1 \rightarrow j'=2$ transition at collision energies of 10 meV and higher.

We now turn to discuss in some detail the spin-averaged cross sections starting from the ortho or para species, irrespective of the final states, i.e., summed over final rotational states j' . Figure 3 shows the overall cross sections for the $7 + \text{o}77(j=0)$ reaction, again plotted as a function of collision energy, including the averaging over nuclear spin functions, as explained in Appendix B. It can be written

$$7 + \text{o}77(j=0) \longrightarrow \begin{cases} 7 + \text{o}77(j') & (\sigma_{j=0 \rightarrow j'}^{\text{oo}}) \\ \text{p}77(j') + 7 & (\sigma_{j=0 \rightarrow j'}^{\text{op}}), \end{cases}$$

and the corresponding cross sections are, here for $j=0$, given by (see Appendix B)

$$\sigma_{j \rightarrow j'} = \begin{cases} \sigma_{j \rightarrow j'}^{\text{oo}} = \frac{4}{9} \sigma_{j \rightarrow j'}^{A_1} + \frac{5}{9} \sigma_{j \rightarrow j'}^E [j' \text{ even}] \\ \sigma_{j \rightarrow j'}^{\text{op}} = \frac{5}{9} \sigma_{j \rightarrow j'}^E [j' \text{ odd}]. \end{cases}$$

Thus, transitions preserving the parity of the (even) rotational quantum number have both A_1 and E components. On the other hand, those for the o-p conversion process are E only. The first feature we notice is that the ICS for the parity conserving reaction is huge, reaching nearly $1000 a_0^2$.

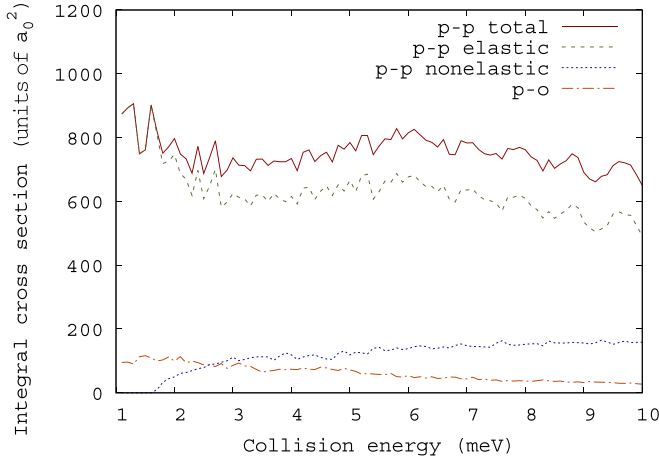


FIG. 4. Spin-averaged initial state selected integral cross sections (in the unit of a_0^2), as a function of collision energy, for the reactive process $7 + p77(j=1)$ with $v=0$.

It oscillates widely but remains 10 to 50 times higher than the o-p one. This is due to the entering of the elastic component for this process. This phenomenon has already been met with the sibling 666 and 888 zero-spin collision systems. Now, as we have seen, here is the additional possibility of o-p nuclear spin isomer conversion, coming exclusively from the existence of nuclear spin for the 777 system. As we can see on the figure, the global o-p process is comparable with the o-o nonelastic one, and at sufficiently low energies, it becomes even more important. However, it also presents a threshold, not visible in Fig. 3, because it occurs at a collision energy lower than 1 meV. It decreases slowly in a quasimonotonic way to reach a value of barely $15 a_0^2$ at higher energies.

Figure 4 shows the exact same observables as in Fig. 3 but for the $7 + p77(j=1)$ reaction;

$$7 + p77(j=1) \longrightarrow \begin{cases} 7 + p77(j') & (\sigma_{j=1 \rightarrow j'}^{pp}) \\ o77(j') + 7 & (\sigma_{j=1 \rightarrow j'}^{po}) \end{cases}$$

and the related cross sections, for $j=1$ here, are now

$$\sigma_{j \rightarrow j'} = \begin{cases} \sigma_{j \rightarrow j'}^{pp} = \frac{2}{9} \sigma_{j \rightarrow j'}^{A_2} + \frac{7}{9} \sigma_{j \rightarrow j'}^E & [j' \text{ odd}] \\ \sigma_{j \rightarrow j'}^{po} = \frac{7}{9} \sigma_{j \rightarrow j'}^E & [j' \text{ even}]. \end{cases}$$

Again, the total p-p process dominates, because of the p-p elastic component. However, if we turn our attention toward the nonelastic ICSs, we notice that the p-p component exhibits a threshold corresponding to the opening of the $j=3$ channel. So, for collision energies up to 1.7 meV, the p-o process, which is exothermic, is the strongest and is of course the only possible reaction at low energies. It then decreases rapidly, as was the case for the $H^+ + H_2$ system, toward nearly the same value as for the o-p reaction described earlier. Finally, if we compare the o-o and p-p processes, we see that the total ICS, as well as the elastic and nonelastic ones, are of the same order of magnitude in both cases. In addition, the global ICS profile is much more structured for o-o than for p-p. This all comes from the elastic component, which presents a highly peaked resonance at an energy slightly less than 2 meV, and many

peaks, ridges, and valleys at higher energies, having survived the partial wave summation.

IV. CONCLUSIONS

To conclude, we have performed a full quantum description of the $^{17}\text{O} + o/p\text{-}^{17}\text{O}$ collision. This peculiar system naturally requires, because of the indistinguishability of the three nuclei, a quantum investigation. We have computed ICSs for an energy range chosen to reveal the different thresholds and numerous resonance structures. A deepened study at very low collision energies would certainly be extremely interesting, but would require the inclusion of magnetic fine-structure coupling parameters in the diatomic Hamiltonian [18,19]. We have witnessed a somewhat interesting spin isomer effect when starting from the diatomic nuclear spin isomer ortho- or para- O_2 . Indeed, the total ICS for parity preserving transitions (ortho-ortho and para-para) is larger and more energy dependent for the $^{17}\text{O} + o\text{-}^{17}\text{O}$ process. On the opposite, the spin-averaged ICSs for ortho-para and para-ortho conversions show a similar behavior, decreasing in a monotonic way with increasing energy. Lastly, we hope that this study will encourage proper use of symmetry arguments when dealing with scattering of indistinguishable entities, especially at low energies.

ACKNOWLEDGMENTS

TIQM calculations were performed using HPC resources from DSI-CCUB (Université de Bourgogne). We thank Richard Dawes for sending us the O_3 PES.

APPENDIX A: SPIN SYMMETRY OF TWO IDENTICAL NUCLEI

As we will need correlations between asymptote entrance channels $^{17}\text{O} + o/p\text{-}^{17}\text{O}$ ($7 + o/p77$) and the whole system $^{17}\text{O}^{17}\text{O}^{17}\text{O}$ (777), that is, between irreducible representations (IRs) of the permutation groups of two and three particles, \mathcal{S}_2 and \mathcal{S}_3 , we briefly recall some facts concerning the diatomic species $^{17}\text{O}^{17}\text{O}$ spin symmetry.

We reproduce for convenience the \mathcal{S}_2 very simple character table, with both \mathcal{S}_2 -Young patterns (shapes or partitions) and C_s -Schönflies-Mulliken notations:

$\mathcal{S}_2 \simeq C_s$	$(\bullet)(\bullet) \simeq e$	$(\bullet\bullet) \simeq \sigma_v$
$[2] \simeq A'$	1	1
$[1^2] \simeq A''$	1	-1

The only two IRs of \mathcal{S}_2 are one-dimensional (\mathcal{S}_2 is Abelian) and noted $[2]$, $\square\square$ or A' and $[1^2]$, \square or A'' . Let s be the spin of ^{17}O ($s=5/2$) nucleus and I be the total nuclear spin of $^{17}\text{O}^{17}\text{O}$ with projection M_I . We can work in coupled representation and define the total spin function of 77 as

$$\phi_{IM_I} = \sum_{m_s} C(ssI; M_I - m_s, m_s) \phi_{sm_s} \phi_{sM_I - m_s}, \quad (\text{A1})$$

where ϕ_{sm_s} are the individual nuclei spin functions and $C(\bullet \bullet \bullet; \bullet, \bullet, \bullet)$ is a Clebsch-Gordan coefficient, with resulting spin quantum numbers taking the integer values $I \in [[0, 2s]]$ and $M_I = -I, -I + 1 \dots + I$. It exhibits a definite parity under the transposition (12) (binary exchange of the two nuclei):

$$(12)\phi_{IM_I} = (-)^{2s-I}\phi_{IM_I}. \quad (\text{A2})$$

Neglecting spin-rotation and spin-spin couplings, the diatom wave function can be written:

$$\Phi = \phi_{el}\phi_{vj}\phi_{IM_I}, \quad (\text{A3})$$

where ϕ_{el} is the $^3\Sigma_g^-$ electronic state (of negative parity) of O_2 and ϕ_{vj} is a rovibrational state, and thus has the parity

$$(12)\Phi = (-)^j(-)^I\Phi = -\Phi. \quad (\text{A4})$$

This permits the classification of the $(2s + 1)^2 = 6^2 = 36$ nuclear spin states of 77 between 21 orthostates o77 ($\phi_{IM_I} \in A', I$ odd and j even) and 15 parastates p77 ($\phi_{IM_I} \in A'', I$ even and j odd). In the case where the atom in the entrance channel is distinguishable, i.e., ^{16}O , we would be in the presence of a process of the form

$$6 + 77 \longrightarrow \begin{cases} 6 + 77 & (\alpha) \\ 67 + 7 & (\beta), \end{cases}$$

with corresponding reactive cross sections given by

$$\sigma_{\alpha v j \rightarrow \beta v' j'} \begin{cases} \frac{7}{12}\sigma_{\alpha v j \rightarrow \beta v' j'}^{A'} [j \text{ even}] \\ \frac{5}{12}\sigma_{\alpha v j \rightarrow \beta v' j'}^{A''} [j \text{ odd}]. \end{cases}$$

APPENDIX B: SPIN SYMMETRY OF THREE IDENTICAL NUCLEI

The starting point is the same as in our previous studies of fully or partly symmetric ozone [30]. As a consequence of the absence of terms involving nuclear or electronic spin in the Hamiltonian describing the system, we write the total wave function of the 777 system as a tensor product:

$$\Psi = \psi_{el}\psi_{\text{nuc.space}}\psi_{\text{nuc.spin}}. \quad (\text{B1})$$

The first factor gathers both the state of motion and spin of electrons. The second part describes the motion of sole nuclei and is of major interest for us. The third part is the nuclear spin function. As required by the Pauli principle, this total wave function Ψ has to belong to the alternating representation of \mathcal{S}_3 , the symmetric (permutation) group of three identical particles. In other words, it must be antisymmetric with respect to binary exchange of any pair of nuclei. The group of importance here, \mathcal{S}_3 , has six elements distributed in three classes, and is isomorphic to D_3 (the group of the equilateral triangle or prism) or the point group C_{3v} of wide use in chemistry. To clarify the upcoming discussion, it is worth reproducing below its simple character table, with both \mathcal{S}_3 -Young patterns and C_{3v} -Schönflies-Mulliken notations:

$\mathcal{S}_3 \simeq C_{3v}$	$(\bullet)(\bullet)(\bullet) \simeq e$	$3(\bullet)(\bullet\bullet) \simeq 3\sigma_v$	$2(\bullet\bullet\bullet) \simeq 2C_3$
$[3] \simeq A_1$	1	1	1
$[1^3] \simeq A_2$	1	-1	1
$[2, 1] \simeq E$	2	0	-1

The totally symmetric representation is the row representation $\begin{array}{|c|c|c|} \hline & & \\ \hline \end{array}$ or A_1 . The alternating representation mentioned

earlier, of capital importance to us, is the column $\begin{array}{|c|} \hline \\ \hline \end{array}$ or A_2 representation.

We note right away that we will have to deal with two-dimensional representations. These are the mixed shape, $\begin{array}{|c|c|} \hline & \\ \hline \end{array}$ or E representations of \mathcal{S}_3 . They arise because the

associated irreducible space (the so-called Specht module) has a basis of two standard polytabloids (column-antisymmetrized row-equivalent classes of Young tableaux) built from two

standard tabloids: $\frac{\begin{array}{|c|c|} \hline 1 & 3 \\ \hline 2 & \end{array}}{2}$ and $\frac{\begin{array}{|c|c|} \hline 1 & 2 \\ \hline 3 & \end{array}}{3}$ themselves originat-

ing from the two possible corresponding standard Young tableaux (see, for example, Ref. [31], Chap. 2).

Now, the collision process $X + X_2 \longrightarrow X + X_2$ under consideration has only one possible final arrangement at moderate collision energies. However, we have two possible entrance channels for this reaction, according to which diatomic spin isomer we consider: $7 + \text{o}77(v, j)$ or $7 + \text{p}77(v, j)$. We therefore have two possible exit channels as well, $7 + \text{o}77(v', j')$ or $7 + \text{p}77(v', j')$. So we will distinguish the two processes:

$$7 + \text{o}77 \longrightarrow \begin{cases} 7 + \text{o}77 & (\alpha) \\ \text{p}77 + 7 & (\beta), \end{cases}$$

$$7 + \text{p}77 \longrightarrow \begin{cases} 7 + \text{p}77 & (\alpha) \\ \text{o}77 + 7 & (\beta). \end{cases}$$

In a general way, the nuclear motion wave function can be decomposed over the inequivalent IRs of \mathcal{S}_3 :

$$\psi_{\text{nuc.space}} \equiv \psi = c_{A_1}\psi^{A_1} + c_{A_2}\psi^{A_2} + c_E\psi^E. \quad (\text{B2})$$

Asymptotically, for a given entrance channel, ϕ_{vj} has a specified initial rotational quantum number j (as well as a vibrational number v). This completely determines the allowed symmetry of $\psi_{\text{nuc.space}}$ of 777 correlating to the entrance channel $7 + \text{o/p}77$. Specifically, in the $7 + \text{o}77$ entrance channel, $\phi_{IM_I} \in A'$ and $\phi_{vj} \in A'$ as well ($j = 0$ and I odd), hence ϕ_{vj} correlates only to A_1 and E , and thus $c_{A_2} = 0$. Therefore,

$$\psi_{\text{nuc.space}} \equiv \psi_o = c_{A_1}\psi^{A_1} + c_E\psi^E. \quad (\text{B3})$$

By the same token, when starting from $7 + p77$, $\phi_{IM_I} \in A''$ and $\phi_{vj} \in A''$ ($j = 1$ and I even), correlating to A_2 and E :

$$\psi_{\text{nuc.space}} \equiv \psi_p = c_{A_2} \psi^{A_2} + c_E \psi^E. \quad (\text{B4})$$

Now what remains to be done is to compute the number of functions of each spin symmetry to get the spin weights associated with the various possible processes. There are several ways to deal with it.

One can work in coupled representation for the three spin angular momenta and use the symmetry properties of Racah coupling coefficients or fractional parentage coefficients. Here again we note s the spin of an individual nucleus. The resulting spin S of the coupled three identical nuclei lies within one of the two subsets: $S \in [[0, 3s]]$ if s is an integer and $S \in [[1/2, 3s]]$ if s is a half-odd integer. So, in our case, with $s = 5/2$, we have $S \in [[1/2, 15/2]]$. This procedure has been used in Ref. [32] and is somewhat cumbersome.

However, as the detailed form of spin functions is not needed (only their numbers in each symmetry), we can use a much simpler device of purely combinatoric nature. The spin vector [or spinor, as it also transforms according to the representations of the $SU(2)$ group] of each particle lies in the $(2s + 1)$ -dimensional vector space V , with basis \mathbf{e}_λ . We will note $d = \dim V = 2s + 1$, that is, $d = 6$ for $s = 5/2$. For a system of three identical particles, the total spin tensor (total spinor) is an element of the tensor space $T^3(V) = V \otimes V \otimes V$. This tensor space splits, under the action of \mathcal{S}_3 , into the subspace of completely symmetric tensors, $P^3(V)$, the subspace of skew-symmetric ones, $\Lambda^3(V)$, and the two remaining subspaces $M^3(V)$ and $\tilde{M}^3(V)$ of mixed symmetry (generated by the Young symmetrizer associated with each of the two standard tableaux of E mentioned earlier—see, for example, Ref. [33], Chap. 20):

$$T^3(V) = P^3(V) \oplus \Lambda^3(V) \oplus M^3(V) \oplus \tilde{M}^3(V). \quad (\text{B5})$$

The total number of spin states is $d^3 = (2s + 1)^3 = 6^3 = 216$. Now the number of spin states of A_1 symmetry is the number, with $\lambda, \mu, \nu \in [[1, d]]$, of completely symmetric monomials $\mathbf{e}_\lambda \otimes \mathbf{e}_\mu \otimes \mathbf{e}_\nu \in P^3(V)$ or, equivalently, the number of completely symmetric components,

$$n_{A_1} = \tau(d, 3) = \binom{d+3-1}{d-1} = \frac{(d+2)!}{(d-1)!3!}, \quad (\text{B6})$$

where $\tau(d, 3)$ is the combination (with multiple occurrences allowed) coefficient of three objects among d . On the other

hand, the number of spin states of A_2 symmetry is given by the usual binomial coefficient:

$$n_{A_2} = \binom{d}{3} = \frac{d!}{(d-3)!3!}. \quad (\text{B7})$$

Finally, the number of states with E symmetry is the remaining number $2n_E = d^3 - n_{A_1} - n_{A_2}$, because E has two dimensions.

So we have, with $d = 6$,

$$n_{A_1} = \frac{(d)(d+1)(d+2)}{6} = \frac{(2s+1)(2s+2)(2s+3)}{6} = 56, \quad (\text{B8})$$

$$n_{A_2} = \frac{(d-2)(d-1)(d)}{6} = \frac{(2s-1)(2s)(2s+1)}{6} = 20, \quad (\text{B9})$$

$$n_E = \frac{(d-1)(d)(d+1)}{3} = \frac{(2s)(2s+1)(2s+2)}{3} = 70, \quad (\text{B10})$$

so $d^3 = n_{A_1} + n_{A_2} + 2n_E$. We are now in a position to calculate the spin weights associated with the various symmetry component cross sections, taking care of the compatibility with the given initial channel.

For the entrance channel $7 + o77$, $w_{A_1} = \frac{n_{A_1}}{n_{A_1} + n_E} = \frac{56}{126} = \frac{4}{9}$ and $w_E = \frac{n_E}{n_{A_1} + n_E} = \frac{70}{126} = \frac{5}{9}$.

On the other hand, for the entrance channel $7 + p77$, $w_{A_2} = \frac{n_{A_2}}{n_{A_2} + n_E} = \frac{20}{90} = \frac{2}{9}$ and $w_E = \frac{n_E}{n_{A_2} + n_E} = \frac{70}{90} = \frac{7}{9}$.

At this point, these spin weights determine the weight of the cross sections (spatial part $\psi_{\text{nuc.space}}$ of the nuclear wave function) by inspection of product representation tables for \mathcal{S}_3 , in such a way that the total wave function Ψ for 777 , including the electronic part ψ_{el} , belongs to A_2 . But if, following Ref. [34], we make the assumption that ψ_{el} is A_2 for any nuclear configuration, as is the case in the asymptotes $7 + 77$, then, for the one-dimensional IRs of \mathcal{S}_3 , we see that the symmetry of $\psi_{\text{nuc.space}}$ must be the same as that of $\psi_{\text{nuc.spin}}$. Consequently, the spin weight just computed is directly applicable to the spatial part. We obtain the factors for E components by a similar reasoning.

In the end, the weighted cross sections for the various allowed collision processes are then, for the reaction $7 + o/p77 \rightarrow 7 + o/p77$,

$$\sigma_{\alpha v j \rightarrow \alpha' v' j'} \begin{cases} \frac{4}{9} \sigma_{\alpha v j \rightarrow \alpha' v' j'}^{A_1} + \frac{5}{9} \sigma_{\alpha v j \rightarrow \alpha' v' j'}^E [j, j' \text{ even}] \\ \frac{2}{9} \sigma_{\alpha v j \rightarrow \beta' v' j'}^{A_2} + \frac{7}{9} \sigma_{\alpha v j \rightarrow \alpha' v' j'}^E [j, j' \text{ odd}] \\ \frac{5}{9} \sigma_{\alpha v j \text{ even} \rightarrow \alpha' v' j' \text{ odd}}^E \\ \frac{7}{9} \sigma_{\alpha v j \text{ odd} \rightarrow \alpha' v' j' \text{ even}}^E \end{cases}$$

[1] C. Janssen, J. Guenther, K. Mauersberger, and D. Krankowsky, *Phys. Chem. Chem. Phys.* **3**, 4718 (2001).
 [2] W. Xie, L. Liu, Z. Sun, H. Guo, and R. Dawes, *J. Chem. Phys.* **142**, 064308 (2015).
 [3] K. Mauersberger, *Geophys. Res. Lett.* **8**, 935 (1981).
 [4] T. R. Rao, G. Guillon, S. Mahapatra, and P. Honvault, *J. Chem. Phys.* **142**, 174311 (2015).
 [5] G. Guillon and P. Honvault, *J. Phys. Chem. A* **120**, 8254 (2016).
 [6] T. R. Rao, G. Guillon, S. Mahapatra, and P. Honvault, *J. Phys. Chem. Lett.* **6**, 633 (2015).
 [7] G. Guillon and P. Honvault, *Chem. Phys. Lett.* **689**, 62 (2017).

[8] G. Guillon, T. R. Rao, S. Mahapatra, and P. Honvault, *J. Phys. Chem. A* **119**, 12512 (2015).
 [9] B. Friedrich, R. deCarvalho, J. Kim, D. Patterson, J. D. Weinstein, and J. M. Doyle, *J. Chem. Soc. Faraday Trans.* **94**, 1783 (1998).
 [10] J. L. Bohn, *Phys. Rev. A* **61**, 040702(R) (2000).
 [11] J. L. Bohn, *Phys. Rev. A* **62**, 032701 (2000).
 [12] A. V. Avdeenkov and J. L. Bohn, *Phys. Rev. A* **64**, 052703 (2001).
 [13] A. Volpi and J. L. Bohn, *Phys. Rev. A* **65**, 052712 (2002).
 [14] A. Volpi and J. L. Bohn, *Phys. Rev. A* **65**, 064702 (2002).

- [15] T. V. Tscherbul, Y. V. Suleimanov, V. Aquilanti, and R. V. Krems, *New J. Phys.* **11**, 055021 (2009).
- [16] J. Pérez-Ríos, J. Campos-Martínez, and M. I. Hernández, *J. Chem. Phys.* **134**, 124310 (2011).
- [17] F. Lique, *J. Chem. Phys.* **132**, 044311 (2010).
- [18] F. Lique, J. Klos, M. H. Alexander, S. D. LePicard, and P. J. Dagdigian, *Month. Not. Astron. Roy. Soc.* **474**, 2313 (2018).
- [19] P. J. Dagdigian, J. Klos, M. Warehime, and M. H. Alexander, *J. Chem. Phys.* **145**, 164309 (2016).
- [20] W. C. Campbell, T. V. Tscherbul, Hsin-I Lu, E. Tsikata, R. V. Krems, and J. M. Doyle, *Phys. Rev. Lett.* **102**, 013003 (2009).
- [21] X.-G. Wang and T. Carrington, *J. Chem. Phys.* **151**, 054101 (2019).
- [22] M. Lepers, B. Bussery-Honvault, and O. Dulieu, *J. Chem. Phys.* **137**, 234305 (2012).
- [23] J. M. Launay and M. LeDourneuf, *Chem. Phys. Lett.* **163**, 178 (1989).
- [24] B. Lepetit and A. Kuppermann, *Chem. Phys. Lett.* **166**, 581 (1990).
- [25] R. Dawes, P. Lolur, A. Li, B. Jiang, and H. Guo, *J. Chem. Phys.* **139**, 201103 (2013).
- [26] B. R. Johnson, *J. Comput. Phys.* **13**, 445 (1973).
- [27] D. E. Manolopoulos, *J. Chem. Phys.* **85**, 6425 (1986).
- [28] G. Cazzoli and C. D. Espoti, *Chem. Phys. Lett.* **113**, 501 (1985).
- [29] P. Honvault, M. Jorfi, T. Gonzalez-Lezana, A. Faure, and L. Pagani, *Phys. Rev. Lett.* **107**, 023201 (2011).
- [30] S. A. Cuccaro, Ph.D. dissertation, California Institute of Technology, 1991.
- [31] B. E. Sagan, *The Symmetric Group—Representations, Combinatorial Algorithms, and Symmetric Functions*, 2nd ed. (Springer, New York, 2001).
- [32] W. H. Miller, *J. Chem. Phys.* **50**, 407 (1969).
- [33] K. S. Lam, *Topics in Contemporary Mathematical Physics*, 2nd ed. (World Scientific, Singapore, 2016).
- [34] C. A. Mead and D. G. Truhlar, *J. Chem. Phys.* **70**, 2284 (1979).